

## CWF18

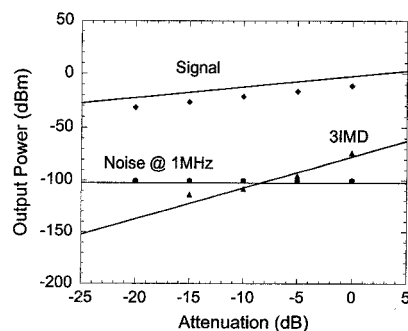
## Dynamic range of DFB semiconductor lasers

J. Chen, R.V. Dalal, R.J. Ram, R. Helkey,\*  
MIT Research Laboratory of Electronics, 77  
Massachusetts Avenue, Room 36-487,  
Cambridge, Massachusetts 02139; E-mail:  
rajeev@mit.edu

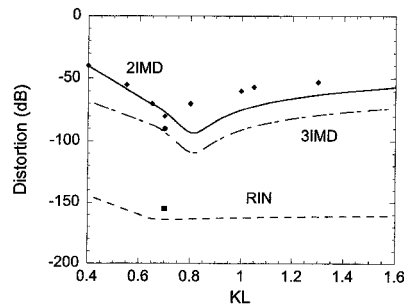
Subcarrier multiplexed systems (SCM) have found widespread application in the delivery of RF signals for cable television, remote radar installations, and recently, for microcellular voice transmission.<sup>1</sup> For broadband applications where cross talk due to laser nonlinearity must be minimized, composite second-order (CSO) and composite triple-beat (CTB) are used to characterize the optical link performance. For high-fidelity, narrowband applications such as radar and microcellular PCS, the important figure of merit is the spurious free dynamic range, which is determined by the largest input RF power for which the intermodulation distortion is below the system noise floor.<sup>2</sup> Modeling the dynamic range of a directly modulated laser requires a high-frequency model of the signal distortion as well as a model for the intensity noise in the laser. This paper presents the first such theoretical analysis of dynamic range in a distributed feedback (DFB) laser. The model is used to analyze the performance of an experimental UHF link and to determine an optimized device design.

Spatially distributed rate equations based on the Green's function method are used to model the nonlinear response and noise of an index-coupled DFB laser.<sup>3</sup> The noise power spectra are determined by introducing the Langevin noise sources into the rate equations. In this way, closed-form expressions for the intermodulation distortion and noise floor can be obtained; this facilitates efficient numerical simulation of DFB performance.

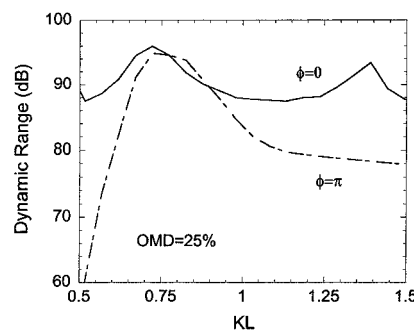
Figure 1 shows the theoretical and experimental RF response and noise as a function of input RF power. The dynamic range is determined by the maximum difference be-



**CWF18 Fig. 1.** The received RF output power at the fundamental frequency, the third-order intermodulation product and the link noise floor for various RF input powers. The lines are calculated from a spatially distributed rate equation model using parameters extracted from ASE spectra and the dots are experimental data for the link described in the text. The laser was biased at  $I = 35$ , mA = 2.2Ith and the two-tone modulation was at 299.5 and 300.5 MHz. The noise floor was measured at a channel bandwidth of 1 MHz.



**CWF18 Fig. 2.** The received RF output power at the second- and third-order intermodulation product and the link noise floor for various  $\kappa L$ . The measured values (dots) are taken from Yonetani *et al.*<sup>4</sup> or from the link measurements reported here. The modulation depth is 25% and the modulation frequencies are 90 and 130 MHz.



**CWF18 Fig. 3.** The calculated dynamic range versus  $\kappa L$  for two values of facet phase at the HR side.  $\phi = 0$  corresponds to lasing on the long-wavelength side and  $\phi = \pi$  corresponds to short-wavelength lasing.

tween the intermodulation distortion and the fundamental output, which produces distortion products smaller than the noise floor. The measurements presented in the plot are from a conventional two-tone modulation scheme for a directly modulated Fujitsu FLD130F3ACH-AL 1.3  $\mu\text{m}$  high-linearity DFB laser. A hybrid- $\pi$  is used to combine the outputs of two isolated signal generators to provide two-tone modulation of the laser.<sup>4</sup> In order to increase the accuracy of the simulation, amplified spontaneous emission spectra from the laser are used to extract various parameters of the DFB lasers.<sup>5</sup> All of the parameters are extracted or fit from cw measurements on the laser diodes. There is no further adjustment made to the model for distortion and noise.

Figure 2 shows the dependence of intermodulation distortion and noise on the normalized coupling coefficient  $\kappa L$  in an HR/AR-coated DFB laser. Spatial hole burning results in a significant contribution to the nonlinear response of the DFB laser. Near  $\kappa L = 0.8$  the DFB laser supports a nearly uniform photon density distribution and hence a minimum intermodulation distortion. The simulations also show that a smaller  $\kappa L$  results in a faster reduction of dynamic range from the maximum value; this occurs because smaller  $\kappa L$  results in increased spatial hole burning as well as increased RIN.

The grating phase ( $\phi$ ) of the HR facet has a significant effect on the analog response of the DFB laser. It not only causes a pronounced change to the photon distribution, but also determines on which side of the Bragg stop band the lasing mode occurs. Lasing on the short wavelength side ( $\phi = 180$ ) results in the highest dynamic range at  $\kappa L = 0.8$ —in agreement with experimental data. However, long-wavelength lasing ( $\phi = 0$ ) results in high dynamic ranges that are less sensitive to variations in  $\kappa L$ . We expect that a  $\kappa L = 0.8$  will result in high yield because of the weak dependence of the dynamic range on grating phase. If long-wavelength lasing can be achieved reliably, there can be an additional improvement in the dynamic range as the bias current is increased. This will be presented along with a discussion of optimal complex grating coefficients for low distortion.

\*MIT Lincoln Laboratory, Lexington, Massachusetts 02173

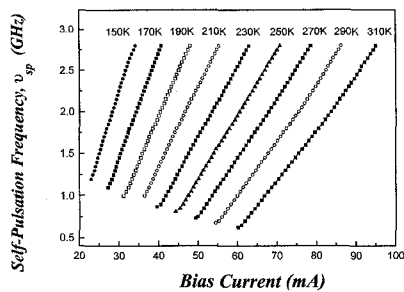
1. C. Cox, E. Ackerman, R. Helkey, G. Betts, to be published in IEEE MTT.
2. H. Roussel, R. Helkey, G. Betts, C. Cox, IEEE Photonics Technol. Lett. **9**, 106 (1997).
3. J. Chen, R. Maciejko, A. Champagne, T. Makino, IEEE J. Quantum Electron. **31**, 1955 (1995).
4. H. Yonetani, I. Ushijima, T. Takada, K. Shima, J. Lightwave Technol. **11**, 147 (1993).
5. W. Feng, A. Hsu, S.L. Chunag, T. Tanbun-EK, A.M. Sergent, IEEE J. Sel. Topics Quantum Electron. **3**, 547 (1997).

## CWF19

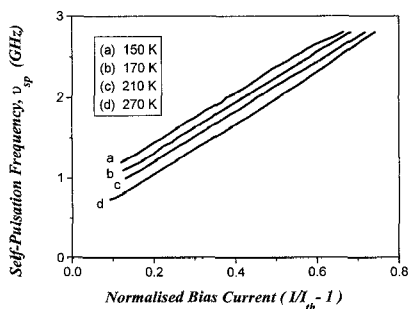
## Effect of temperature on self-pulsation in narrow stripe, gain-guided, compact disk laser diodes

S. Lynch, P. McEvoy, P. Landais,  
J. O'Gorman, D. McDonald, J. Hegarty,  
Physics Department, Trinity College, Dublin 2,  
Ireland

There is an ongoing strong interest in the development of red self-pulsating lasers for data storage compact disk (CD) applications.<sup>1</sup> Of particular importance in this mass-market application is that the laser diode emission exhibits strong self-pulsation over an extended temperature range (0–80°C), since control of the device temperature is mitigated by the low costs required for this application. It is widely believed that carrier transport and recombination play a significant role in the temperature dependence of the self-pulsation, since self-pulsation in these CD laser structures arises from a delicate interplay between the spatially nonuniform inversion of the semiconductor material and the photons circulating in the laser cavity. This interplay, however, is not well understood. In order to gain some insight on the self-pulsation process in CD gain-guided devices we have examined the temperature dependence of self-pulsation in commercial CD lasers emitting at  $\lambda = 800$  nm, which are used in current storage applications. Since these devices reliably self-pulsate over the range 0–80°C, we have examined their behavior



CWF19 Fig. 1. Self-pulsation frequency (GHz) as a function of bias current (mA), parameterized in terms of temperature (K).



CWF19 Fig. 2. CD laser diode self-pulsation frequency as a function of normalized bias current for a range of heat sink temperatures (150 K, 170 K, 210 K, 270 K—upper curve to lower).

from cryogenic temperatures (77 K) to above room temperature (310 K).

The temperature dependence of self-pulsation in a SHARP LT022MD CD laser diode was measured in the range 77 to 310 K. Self-pulsation was found to occur down to approximately 100 K. Here, we present detailed measurements of the variation of self-pulsation frequency with bias current in the temperature range 150 to 310 K (Fig. 1). The self-pulsation frequency ( $\nu_{sp}$ ) was found to vary more rapidly with bias current as the heat sink temperature decreases. When this data is replotted (Fig. 2.) in the more conventional form,  $\nu_{sp}$  versus normalized bias current ( $I/I_{th} - 1$ ), it is clear that the slope of these curves are not strongly temperature dependent. Furthermore the variation of  $\nu_{sp}$  with  $(I/I_{th} - 1)$  clearly shows a linear and not a square root dependence. This result is interesting since it is commonly assumed that the self-pulsation frequency in CD laser structures occurs at the laser diode modulation resonance frequency, which is often described by the relationship:

$$\Omega_R = \left[ \frac{1}{\tau_e \tau_p} \left( \frac{I}{I_{th}} - 1 \right) \right]^{1/2}$$

where  $\Omega_R$  is the relaxation oscillation frequency,  $\tau_e$  and  $\tau_p$  are the carrier and photon lifetimes,  $I$  is bias current and  $I_{th}$  is the threshold bias current. This relationship predicts a quadratic dependence of normalized bias current on  $\Omega_R$  and a temperature dependence of the slope due to the well-known temperature dependence of carrier lifetime, neither of which is apparent from Fig. 2.

We explain these phenomena using a stan-

standard rate equation model and simple physical approximations to describe the temperature variance of gain, carrier lifetime, carrier diffusion, and optical mode shape. These calculations agree well with experiment and shed light on the interplay that occurs between these physical effects that are required to create a sustained self-pulsating emission in these structures. These results can be applied to the problem of developing laser diodes with short wavelength emission for data storage applications that exhibit strong self-pulsation over an extended temperature range.

1. H. Adachi, S. Kamiyama, I. Kidoguchi, T. Uenoyama, IEEE Photonics Technol. Lett. 7(12) (1995).
2. G.P. Agrawal, N.K. Dutta, *Long Wavelength Semiconductor Lasers* (Van Nostrand Reinhold Electrical/Computer Science and Engineering Series, 1986).

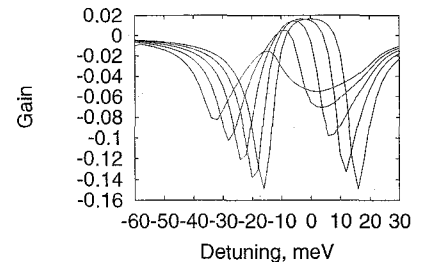
## CWF20

### Many-body theory of quantum interference effects in semiconductor quantum well lasers

Dmitri E. Nikonov, Ataç Imamoğlu, Holger Schmidt, Marlan O. Scully,\*  
Department of Electrical and Computer Engineering and Center for Quantized Electronic Structures (QUEST), University of California, Santa Barbara, California 93106-9560

Collective excitations resulting from the Coulomb interaction of electrons and holes are known to determine the spectrum of gain or absorption for semiconductor lasers in interband transitions.<sup>1</sup> In view of the progress of intersubband lasers,<sup>2</sup> the proposal of lasers without population inversion (LWI) in intersubband transitions<sup>3</sup> was made. It is based on the absorption cancellation via Fano interference of tunneling processes. Tunneling-induced transparency was recently observed in such schemes.<sup>4,5</sup> For the demonstration of LWI in semiconductors, it is crucial to reveal the role of collective excitations and inhomogeneous broadening.

We consider a scheme with two closely spaced upper subbands  $a$  and  $a'$  and a lower subband  $b$  within the conduction band of a multiple quantum well.<sup>3</sup> The electrons are injected into and removed out of the subbands due to tunneling between the wells and quasi-continuum regions surrounding them. The tunneling involving the upper subbands experience Fano interference of two incoherent processes, which induces coherence between them and enables absorption cancellation. We calculate gain via the solution of semiconductor Bloch equations,<sup>1</sup> which allows us to account for the Coulomb interaction between electrons. The effective masses are different in the subbands, and this results in a subband dispersion: transitions between different momenta of electrons have different resonant energies, or, in other words, the transition is inhomogeneously broadened. We find that the Coulomb interaction causes formation of collective modes ("repellons") associated with the Fermi-edge singularity of the repelling pairs of an electron in the  $a$  subband and a hole in the  $b$



CWF20 Fig. 1. Gain as a function of detuning with injection to the upper subbands  $r_a = 2$  meV and decay  $\gamma_a = 3$  meV for  $m_a = 0.042, 0.037, 0.033, 0.03, 0.028 m_0$  in the order of the gain maximum shifting to the left.

subband. The broadening of repellons is homogeneous and is much smaller than the inhomogeneous broadening due to single-particle modes. Large inhomogeneous broadening is known to destroy LWI.

Figure 1 shows the results of the numerical simulation of the gain as a function of the detuning of the laser field for different values of the subband dispersion. Gain is exhibited in a narrow region close to the resonance surrounded by the regions of absorption, which implies the absence of inversion. The calculations without the account of Coulomb interaction would predict no gain. This allows us to conclude that this one of the few examples of Fano interference of collective modes is the only explanation of LWI. Gain disappears at still larger inhomogeneous broadening, but the tunneling-induced transparency dip is still pronounced.

\*Department of Physics, Texas A&M University, College Station, Texas 77843-4242

1. W.W. Chow, S.W. Koch, M. Sargent III, *Semiconductor-Laser Physics* (Springer-Verlag, Berlin, 1993).
2. J. Faist *et al.*, Nature **387**, 777 (1997).
3. A. Imamoğlu, R.J. Ram, Opt. Lett. **19**, 1744 (1994).
4. H. Schmidt, K.L. Campman, A.C. Gosard, A. Imamoğlu, Appl. Phys. Lett. **70**, 3455 (1997).
5. J. Faist *et al.*, Opt. Lett. **21**, 985 (1997).

## CWF21

### Heating of high-power laser diode arrays: from temperature data to power management and failure mechanisms

J.W. Tomm, A. Bärwolff, R. Puchert, A. Jaeger, Ch. Lienau, T. Elsaesser, Max-Born-Institut für Nichtlineare Optik und Kurzzeitspektroskopie, Rudower Chaussee 6, D-12489 Berlin, Germany

High-power laser diode arrays (LDA) are important radiation sources for a number of applications. Device operation usually happens under heavy thermal load. Thus for reducing failure sensitivity, detailed insight into the power balance of the devices is of great importance.

Temperature data from the devices during operation are obtained by a number of optical techniques such as micro-Raman spectroscopy (facet heating), laser emission data (bulk heat-